15 Jun 2020

Channel Estimators for Full-Duplex Communication using Orthogonal Pilot Sequences

Arul Mathi Maran Chandran

Lei Wang

Maciej Jan Zawodniok
Missouri University of Science and Technology, mjzx9c@mst.edu

Recommended Citation

A. M. Chandran et al., "Channel Estimators for Full-Duplex Communication using Orthogonal Pilot Sequences," *IEEE Access*, vol. 8, pp. 117706-117713, Institute of Electrical and Electronics Engineers (IEEE), Jun 2020.
The definitive version is available at https://doi.org/10.1109/ACCESS.2020.3002726

IEEE Access
Multidisciplinary | Rapid Review | Open Access Journal

Received May 6, 2020, accepted June 8, 2020, date of publication June 15, 2020, date of current version July 7, 2020.

Digital Object Identifier 10.1109/ACCESS.2020.3002726

Channel Estimators for Full-Duplex Communication Using Orthogonal Pilot Sequences

ARUL MATHI MARAN CHANDRAN[1], (Graduate Student Member, IEEE), LEI WANG[2], (Member, IEEE), AND MACIEJ ZAWODNIOK[1], (Senior Member, IEEE)

[1]Department of Electrical and Computer Engineering, Missouri University of Science and Technology, Rolla, MO 65409, USA
[2]Department of Computer Science and Computer Engineering, University of Wisconsin–La Crosse, La Crosse, WI 54601, USA

Corresponding author: Arul Mathi Maran Chandran (ac62f@mst.edu)

This work was supported in part by the Intelligent Systems Center (ISC), Missouri University of Science and Technology, Rolla, MO, USA.

ABSTRACT Full-duplex communication is desirable to maximize the spectral efficiency, despite the challenges it puts forth. The key challenge inhibiting the operation of radios in full-duplex mode is self-interference. In this paper, we propose a pilot-based channel estimation to estimate both self-interference and communication channels simultaneously at both ends of a full-duplex link using orthogonal sequences. The Cramer-Rao Lower Bound for estimators of both the channels was determined and compared with the half-duplex channel estimator. We performed simulations varying sequence length and channel taps and studied the performance of the estimators. We also studied the effect of synchronization between the sequences on the performance of the estimators. Thus, providing a solution to balance the trade-off between the accuracy of the channel estimation and the overhead added to the transmissions for full-duplex communication.

INDEX TERMS Channel estimation, orthogonal m-sequences, full-duplex (FDX), half-duplex (HDX), self-interference (SI), Cramer-Rao lower bound (CRLB).

I. INTRODUCTION

Rapid evolution in telecommunication and increasing population penetration demands more bandwidth to support new users in addition to the existing users with reliable high-speed data services. Most existing technologies operate in half-duplex (HDX) mode by performing only transmission or reception at any instance of time, achieving only fifty percent of the spectral efficiency. The full-duplex (FDX) mode of operation where the transmission and reception are performed simultaneously which can potentially achieve double the spectral efficiency of the existing mode of operation. Thus, FDX mode proves to be a promising solution for future wireless systems. FDX also provide solutions faced by the existing HDX operations such as a hidden terminal, throughput bottlenecks due to congestion, large end-to-end delays [1]. There are existing applications that deploy FDX operations, especially in relay systems. The use of FDX in relay systems increases the coverage and throughput. FDX is been considered a potential solution in the next-generation telecommunication technologies such as 5G [2], Non-orthogonal multiple access (NOMA) [3]–[7].

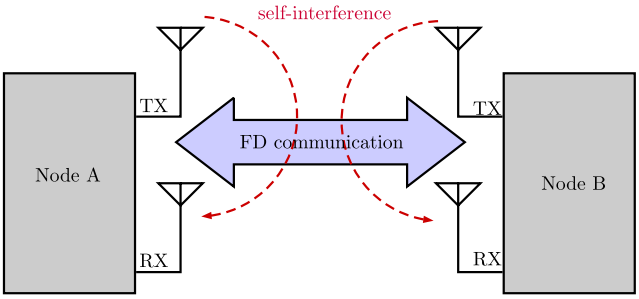

FIGURE 1. Block diagram of full-duplex operation.

The major challenge of FDX operation is rooted in its operation. Since transmission and reception occur simultaneously, the transmitted signal interferes with its own receiver's operation. This is called self-interference (SI)

The associate editor coordinating the review of this manuscript and approving it for publication was Parul Garg.

which affects the throughput and potentially degrading the communication. In addition to the reflection of the transmitted signal, SI also occurs across the transmitter and receiver chain within the radio. To harness the benefits of FDX, suppression/cancellation of SI is necessary. Since the SI signal strength is high compared to the weak desired signal, multiple stages of SI cancellation both in analog and digital have been proposed in the literature. Though full-duplex is considered a potential methodology in the next-generation systems, the lack of a feasible solution to estimate and mitigate self-interference lost its appeal to adopt in commercial mobile applications. Instead, the industry sought to move towards higher frequencies of operation to meet the demand. There is an increased interest to operate in a non-licensed band such as LTE-U, LTE-LAA. Unfortunately, operating in high-frequency bands such as millimeter operations also pose challenges such as shorter range, limited mobility, channel modeling [8].

The estimation of SI channel coefficients plays a vital role in the mitigation of self-interference. To achieve the best estimation possible, we should able to separate the SI and communication channel components at the reception. This separation can be achieved by orthogonality which already used in code-division multiple access (CDMA) and orthogonal frequency division multiplexing (OFDM) which operates in HDX mode. The signals orthogonal to each other do not interfere with each other and can be evaluated separately without the influence of the other. Generally, the channels are estimated using known pilot sequences, and the orthogonal sequences are proposed to be used as a pilot sequence to estimate SI and communication channel.

The contribution of this paper is as follows. We proposed the system model and defined the correlation properties of both autocorrelation and cross-correlation requirements for the sequences to be used as pilot sequences in the proposed method. We proposed to use a set of selected orthogonal m-sequences which are closely compliant with the expected correlation properties as orthogonal pilot sequences to achieve separation and estimation of SI and communication channels. We also determined the Cramer-Rao Bound of the estimators for full-duplex operations and compared them with the half-duplex operations.

The paper is organized as follows. Section II discuss the various existing works to achieve full-duplex operation. Section III describes briefly the system model proposed and the proposed method to use the orthogonal m-sequence as pilots to estimate both the SI and communication channels. We also briefly discussed the effect of synchronization offset in the performance of the estimators. The CRLB of the proposed method is formulated in section IV. Finally, section V discuss the simulation and results of the proposed methodology.

A. NOTATIONS

The matrices are denoted by upper-case letters and the vectors by lower-case letter with a macron. $(\cdot)^T$, $(\cdot)^H$, and $E(\cdot)$ denotes transpose, hermitian, expectation operations respectively. $\mathcal{CN}(\mu, \sigma^2)$ denotes complex Gaussian distribution with mean μ and variance σ^2.

II. RELATED WORKS

In this section, we discuss the related works from the literature on the solutions to suppress and mitigate self-interference during FDX operation. The proposed work improves on the existing works by optimizing the accuracy of the channel estimation while minimizing the overhead.

Most of the works in the literature consider relay systems [9], [10] for FDX operations. In the relay systems, only the relaying nodes operate in FDX mode forwarding the received signal to the next communication link and all other nodes operate in HDX mode. FDX operation finds its application in relay nodes since they are stationary and physically able to isolate transmitter and receiver. Therefore, the effects of self-interference are considered negligible. In more general scenarios, the effects of SI are significant in FDX operation and must be addressed. The target solution for an effective FDX operation is to estimate and mitigate the self-interference caused by the transmitter. A theoretical analysis was performed and showed that for a bidirectional communication system with multiple antennas, FDX can be more efficient than HDX even with channel estimation error [11].

The critical step to mitigate the effects of SI channel from the received signal is to estimate the SI channel coefficients. Different estimators are proposed for FDX systems to estimate the SI channel and perform cancellation at different stages of data recovery. The suppression of self-interference is addressed at different stages of processing both in analog [12]–[18], and digital domains [19]–[27]. An additional receiver chain was proposed [12] to obtain a reference signal for digital SI cancellation. The analog cancellation techniques do not remove 100% of the SI signal. However, analog cancellation techniques are necessary to reduce the SI signal strength down to an acceptable range of the transceiver to continue further cancellation in the digital domain. The proposed method in this paper is performed in the digital domain after the received signal strength is reduced to the operational level of the digital domain by analog cancellation using one of the solutions listed above.

The residual SI signal reaching the digital domain is significant enough to affect the performance of decoding the signal of interest. Hence, the residual SI cancellation must be performed in the digital domain to improve the performance of the FDX operation. The characterization of the distribution of the SI before and after cancellation mechanisms and the effect of performing digital cancellation after analog cancellation is discussed in [19]. A design prototype and implementation of full-duplex operation using Wi-Fi radios were presented in a constrained indoor environment, presenting the throughput values closer to the expected theoretical doubling of spectral efficiency in [1], [20].

There are different methods proposed in the literature to estimate the self-interference. The use of an auxiliary receiver

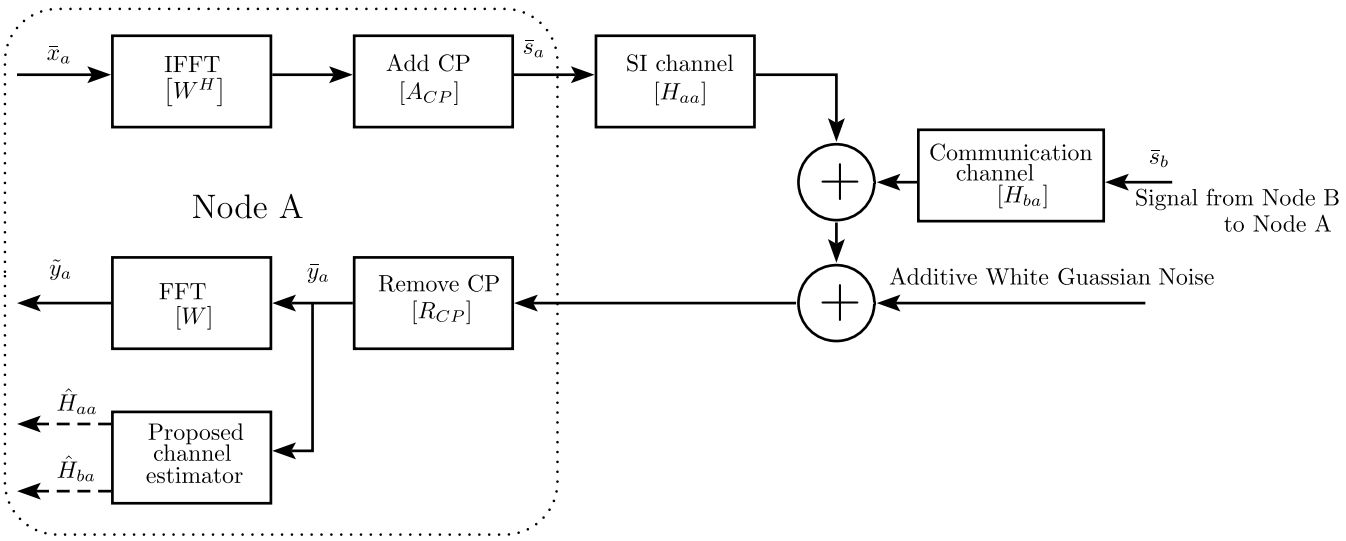

FIGURE 2. Block diagram of OFDM system with the proposed method for full-duplex operation.

is one of the common approaches towards the estimation of the SI channel. A Kalman filter is used to estimate the SI channel from a copy of the transmitted signal via an auxiliary receiver in [28]. The joint estimation of the SI channel and communication channel using the ML criterion was presented in [25]. The estimation exploits the known transmitted signal from the auxiliary receiver and second-order statistics of the unknown signal for the identification of respective channels. These techniques focus on the SI cancellation but lack the effect of SI cancellation on the signal-of-interest and the dynamicity of the channels. Recently, there is a proposed work in the literature to separate pilots from different nodes by placing the pilots in non-overlapping time slots [29].

The solution we propose improves the channel estimation for both SI and communication channels by employing known orthogonal sequences as pilots which can be transmitted simultaneously. These sequences remove the uncertainty to distinguish pilots from the received signal using the orthogonality property. The orthogonality property of these sequences is already being used in various applications such as MIMO [30]–[32] for channel estimation, to reduce pilot contamination in cellular cells [31], [32], in detection algorithms to provide robustness against eavesdroppers [33], scramble and accommodate multiple users transmission simultaneously.

III. FULL-DUPLEX OPERATION

In this section, we discuss the proposed method to operate an OFDM system in full-duplex mode and discussed the desired correlation properties of the sequences for the proposed method. In the following discussions, we considered two nodes A and B communicate in full-duplex mode. The discussion of the proposed method considers the reception at node A, which is also applicable to node B. The proposed method is performed in the digital domain after analog cancellation which reduces the received signal to the operational range of the digital domain. The analog cancellation techniques in the literature as listed in the earlier section show potential suppression to perform digital cancellation to remove the residual self-interference and shown it is effective by performing digital cancellation after analog cancellation [19].

A. PROPOSED METHOD

The block diagram of the OFDM operating in FDX mode considered for the proposed method is shown in Fig. 2. Both the nodes A and B operate in FDX mode and at the reception of node A signals from both node A and node B are received. The channel effect on these signals is independent.

Considering an OFDM system with L equispaced subcarrier and cyclic prefix of length L_{CP} forming an OFDM block of length, N. The symbol sequence contains both the data and pilot symbols. In general, the receivers may use the pilot symbols for synchronization in time and frequency, offset correction, estimate the channel, etc. The OFDM block transmitted in the k^{th} block is given by

$$s[k] = A_{CP} W^H x[k], \tag{1}$$

where, $x[k]$ is the symbols of length L to be transmitted containing the data and pilot symbols. A_{CP} is the $N \times L$ matrix which insert the cyclic prefix of length L_{CP} and W is the $L \times L$ unitary discrete Fourier transform (DFT) matrix whose elements are given by $W_{mn} = (1/L)\, exp\,(-j2\pi mn/L)$, $0 \geq (m, n) \leq L - 1$.

Then, the received symbols at the reception of node A is given by

$$\bar{r}_a[k] = H_{aa}[k]\bar{s}_a[k] + H_{ba}[k]\bar{s}_b[k] + \bar{\eta}[k], \tag{2}$$

where, s_a and s_b are the symbol vectors transmitted by the nodes A and B respectively. H_{aa} and H_{ba} are the SI and communication channels at the receiver of node A.

After removing the cyclic prefix for pilot slot,

$$\begin{aligned}\bar{y}_a &= R_{CP}\left(\bar{r}_a\right)\\ &= R_{CP}H_{aa}A_{CP}W^H\left(W\bar{x}_{pa}\right)\\ &\quad +R_{CP}H_{ba}A_{CP}W^H\left(W\bar{x}_{pb}\right)+\bar{\eta}\\ &= R_{CP}H_{aa}A_{CP}\left(W^HW\right)\bar{x}_{pa}\\ &\quad +R_{CP}H_{ba}A_{CP}\left(W^HW\right)\bar{x}_{pb}+\bar{\eta}\\ &= H_{at}\bar{x}_{pa}+H_{bt}\bar{x}_{pb}+\bar{\eta}\\ &= X_{pa}\bar{h}_{at}+X_{pb}\bar{h}_{bt}+\bar{\eta}. \end{aligned} \tag{3}$$

To remove the SI channel component from (3), multiply X_{pb}^T on both sides of the equation as shown in (4).

$$X_{pb}^T\bar{y}_a = X_{pb}^TX_{pa}\bar{h}_{at}+X_{pb}^TX_{pb}\bar{h}_{bt}+X_{pb}^T\bar{\eta} \tag{4}$$

$$= 0_L+I_L\bar{h}_{bt}+X_{pb}^T\bar{\eta} \tag{5}$$

$$\left[\because X_{pb}^TX_{pa}=0_L; X_{pb}^TX_{pb}=I_L\right]$$

$$= \bar{h}_{bt}+X_{pb}^T\bar{\eta}, \tag{6}$$

where 0_L is zero matrix and I_L is identity matrix of size L. Similarly, the SI channel component can be extracted from (3), multiply X_{pa}^T on both sides of the equation as shown in (7).

$$X_{pa}^T\bar{y}_a = X_{pa}^TX_{pa}\bar{h}_{at}+X_{pa}^TX_{pb}\bar{h}_{bt}+X_{pa}^T\bar{\eta} \tag{7}$$

$$= I_L\bar{h}_{at}+0_L+X_{pa}^T\bar{\eta} \tag{8}$$

$$\left[\because X_{pa}^TX_{pb}=0_L; X_{pa}^TX_{pa}=I_L\right]$$

$$= \bar{h}_{at}+X_{pa}^T\bar{\eta}. \tag{9}$$

From equations (6) and (9), the maximum likelihood estimate of the communication and SI channel estimates can be written as

$$\tilde{h}_{bt} = X_{pb}^T\bar{y}_a, \tag{10}$$

$$\tilde{h}_{at} = X_{pa}^T\bar{y}_a. \tag{11}$$

B. SYNCHRONIZATION

In addition to self-interference, synchronization between the two channels is another key issue to be considered in full-duplex communication. The SI signal and the signal of interest is not necessarily aligned at the reception. The offset between the SI signal and the signal of interest at the reception, depends on the propagation delay between the nodes and the reflections from the environment. The effect of propagation delay is propositional to the distance between the nodes. For short range communication, this effect is minimum to negligible well below the tolerance of the system. For example, OFDM suffers from inter-Carrier-interference when timing variance of the channel during one OFDM symbol interval affects the orthogonality and results in power leakage among the subcarriers.

In the proposed method, this offset can be measured from the correlation peaks of the orthogonal sequences. The correlation yields two peaks aligned to respective orthogonal sequences of the nodes. This offset can be tracked and used to compensate at the mitigation of the channel effects at the equalization for both SI and communication channel. The tolerance depends on the correlation property once it overlaps with data signal in the other channel. The scope of this paper does not include the synchronization and all results discussed are with synchronized SI signal and signal of interest at the reception.

C. SELECTION OF THE PSEUDO RANDOM SEQUENCES

The desired correlation properties of the orthogonal sequence are (a) the autocorrelation of the sequence should have its peak only with its zero shifted version and zero for all other linear shifts, (b) the cross-correlation of the sequence with any other sequence should be zero as shown in (12) and (13).

$$r_{xx}(\tau) = \begin{cases} 2^N, & \text{if } \tau = 0,\\ 0, & \text{if } \tau \neq 0 \end{cases}, \tag{12}$$

$$r_{xy}(\tau) = 0, \quad \forall\tau. \tag{13}$$

The orthogonal sequence with the correlation properties as mention in (12) and (13) is not available in the literature. The cross-correlation of the orthogonal sequences is zero, but their autocorrelation varies with one or more peaks with non-zero values for different shifts. These variations in the autocorrelation of the sequences introduce error to the estimation. The sequences with the correlation properties closed to the requirements are orthogonal m-sequence. The Gold and Kasami sequences are not suitable candidates because their autocorrelation is not two-valued and not as good as that of m-sequences. The orthogonal Walsh sequence does not match the requirement since the autocorrelation swings between positive peak $(+1)$ and negative peak (-1) across even and odd shifts respectively.

The autocorrelation of the m-sequence of length N is given by

$$r_{xx}(j) = \begin{cases} N, & \text{if } j = 0,\\ -1, & \text{if } 1 \leq j \geq N-1 \end{cases} \tag{14}$$

and the cross-correlation in general may have large peaks which can be exhibited as three-valued cross-correlation with values $\{-1, -t(n), t(n)-2\}$, where

$$t(n) = \begin{cases} 2^{\frac{(n+1)}{2}}+1, & \text{if n is odd}\\ 2^{\frac{(n+2)}{2}}+1, & \text{if n is even} \end{cases} \tag{15}$$

The preferred orthogonal m-sequences are the ones with the closest correlation properties for the proposed method to separate and estimation individual channel coefficients.

The m-sequence defined in [34] whose properties are closer to the desired properties is chosen for the proposed method. The orthogonal m-sequence is derived from the m-sequence whose length is 2^M-1, where M is a positive integer. The length of the orthogonal m-sequence is 2^M and the sequences are binary sequences $\in [-1, +1]$.

IV. CRLB FOR THE PROPOSED METHOD

In this section, we derive the Cramer-Rao Lower Bound (CRLB) of the channel estimators both SI and communication channels for the proposed method.

$$\bar{y}_a = X_{pa}\bar{h}_{at} + X_{pb}\bar{h}_{bt} + \bar{\eta}, \tag{16}$$

where, $\bar{h}_{at}$ and $\bar{h}_{bt}$ are channel coefficient of the SI and the communication channel. These two parameters are the parameters of interest to be estimated which is indicated by $\bar{\theta} = \left[\bar{h}_{at}\ \bar{h}_{bt}\right]^T$.

The probability density function of the received slot with N symbols is given by

$$p(\bar{y_a}, \bar{\theta}) = \frac{1}{\left(2\pi\sigma^2\right)^{\frac{N}{2}}} \times exp\left[\frac{-1}{2\sigma^2}\left\|\bar{y}_a - X_{pa}\bar{h}_{at} + X_{pb}\bar{h}_{bt}\right\|^2\right]. \tag{17}$$

To determine the CRLB of the estimator, the Fisher information matrix $\mathbf{I}(\bar{\theta})$ must be evaluated which is given by

$$\mathbf{I}(\bar{\theta}) = \begin{bmatrix} -E\left[\frac{\partial^2 \ln p(\bar{y_a}, \bar{\theta})}{\partial h_{at}^2}\right] & -E\left[\frac{\partial^2 \ln p(\bar{y_a}, \bar{\theta})}{\partial h_{at}\partial h_{bt}}\right] \\ -E\left[\frac{\partial^2 \ln p(\bar{y_a}, \bar{\theta})}{\partial h_{bt}\partial h_{at}}\right] & -E\left[\frac{\partial^2 \ln p(\bar{y_a}, \bar{\theta})}{\partial h_{bt}^2}\right] \end{bmatrix}. \tag{18}$$

Recall that for the estimation of vector parameter, $\bar{\theta} = [\theta_1\ \theta_2\ \ldots\ \theta_n]^T$. If $\hat{\theta}_i$ is an unbiased estimator, then the CRLB of $\hat{\theta}_i$ is ii^{th} element of the inverse of the Fisher information matrix [35], $\mathbf{I}(\bar{\theta})$

$$var(\hat{\theta}_i) \geq \left[\mathbf{I}^{-1}(\bar{\theta})\right]_{ii}. \tag{19}$$

Now, we evaluate the individual element of the Fisher information matrix. The logarithm of the probability density function of the reception is

$$\ln p(\bar{y_a}, \bar{\theta}) = \frac{-N}{2}\ln(2\pi\sigma^2 I) \times \frac{-1}{2\sigma^2 I}\left\|\bar{y}_a - X_{pa}\bar{h}_{at} + X_{pb}\bar{h}_{bt}\right\|^2, \tag{20}$$

and expanding the contents within the norm square yields

$$\bar{y_a}^H\bar{y_a} - 2\bar{h}_{at}^H X_a^H\bar{y_a} - 2\bar{h}_{bt}^H X_b^H\bar{y_a} + 2\bar{h}_{at}^H X_a^H X_b\bar{h}_{bt} + \bar{h}_{at}^H X_a^H X_a\bar{h}_{at} + \bar{h}_{bt}^H X_b^H X_b\bar{h}_{bt}. \tag{21}$$

Then, the partial derivatives of (20) using (21) to build the Fisher information matrix are given by

$$\frac{\partial \ln p(\bar{y_a}, \bar{\theta})}{\partial \bar{h}_{at}} = \frac{-1}{\sigma^2 I}\left[-2X_a^H\bar{y_a} + 2X_a^H X_b\bar{h}_{bt} + X_a^H X_a\bar{h}_{at}\right],$$

$$\frac{\partial \ln p(\bar{y_a}, \bar{\theta})}{\partial \bar{h}_{bt}} = \frac{-1}{\sigma^2 I}\left[-2X_b^H\bar{y_a} + 2X_b^H X_b\bar{h}_{bt} + X_b^H X_b\bar{h}_{bt}\right],$$

$$\frac{\partial^2 \ln p(\bar{y_a}, \bar{\theta})}{\partial \bar{h}_{at}^2} = \frac{-1}{\sigma^2 I}\left[X_a^H X_a\right], \tag{22}$$

$$\frac{\partial^2 \ln p(\bar{y_a}, \bar{\theta})}{\partial \bar{h}_{bt}^2} = \frac{-1}{\sigma^2 I}\left[X_b^H X_b\right], \tag{23}$$

$$\frac{\partial^2 \ln p(\bar{y_a}, \bar{\theta})}{\partial \bar{h}_{bt}\partial \bar{h}_{at}} = \frac{-1}{\sigma^2 I}\left[2X_a^H X_b\right], \tag{24}$$

$$\frac{\partial^2 \ln p(\bar{y_a}, \bar{\theta})}{\partial \bar{h}_{bt}\partial \bar{h}_{at}} = \frac{-1}{\sigma^2 I}\left[2X_a^H X_b\right]. \tag{25}$$

Now using (22),(24), (25, and (23)) in (18), then the Fisher information matrix can written as

$$\mathbf{I}(\bar{\theta}) = \frac{1}{\sigma^2 I}\begin{bmatrix} E\left[X_a^H X_a\right] & E\left[2X_b^H X_a\right] \\ E\left[2X_a^H X_b\right] & E\left[X_b^H X_b\right] \end{bmatrix}. \tag{26}$$

Inverting the Fisher information matrix from (26) yields

$$\mathbf{I}(\bar{\theta})^{-1} = \frac{\sigma^2 I}{D}\begin{bmatrix} E\left[X_b^H X_b\right] & -E\left[2X_b^H X_a\right] \\ -E\left[2X_a^H X_b\right] & E\left[X_a^H X_a\right] \end{bmatrix}. \tag{27}$$

where, D is the determinant of the Fisher information matrix given by

$$D = E\left[X_a^H X_a\right].E\left[X_b^H X_b\right] - E\left[2X_a^H X_b\right].E\left[2X_b^H X_a\right].$$

The variance of the parameter also the Cramer-Rao bound of the $\bar{h}_{at}$ and $\bar{h}_{bt}$ are the diagonal elements of the inverse Fisher information matrix (19) using (27) are

$$var(\bar{h}_{at}) \geq \frac{\sigma^2 I}{D}E\left[X_b^H X_b\right], \tag{28}$$

$$var(\bar{h}_{bt}) \geq \frac{\sigma^2 I}{D}E\left[X_a^H X_a\right]. \tag{29}$$

Furthermore (28) and (29) can be simplified for the orthogonal sequence whose cross-correlation is zero $\left[X_a^H X_b = X_b^H X_a = 0\right]$ and assuming perfect autocorrelation where $E\left[X_a^H X_a\right] = E\left[X_b^H X_b\right] = NI$, the variance of the estimators can be written as

$$var(\bar{h}_{at}) \geq \frac{\sigma^2 I}{E\left[X_a^H X_b\right]} \geq \frac{\sigma^2}{N}, \tag{30}$$

$$var(\bar{h}_{bt}) \geq \frac{\sigma^2 I}{E\left[X_b^H X_b\right]} \geq \frac{\sigma^2}{N}. \tag{31}$$

From (30) and (31), the bound depend on the autocorrelation of the orthogonal sequence. Lower the autocorrelation, the variance of the estimators' increases which yields lower performance in the estimation of the channel parameters. The results also match the variance of the channel estimator in a half-duplex communication.

V. RESULTS

In this section, we discuss and analyze different simulation results for the proposed method.

The autocorrelation and cross-correlation of the orthogonal sequence are shown in Fig. 3. The cross-correlation of the selected orthogonal m-sequence is zero with any other sequence. The autocorrelation is non-zero with most of its linear shifts. The maximum peak occurs only when correlated with itself without any linear shift. The non-zero autocorrelation of the orthogonal sequence will introduce error since it does not yield an identity matrix in (5) and (8). For a given

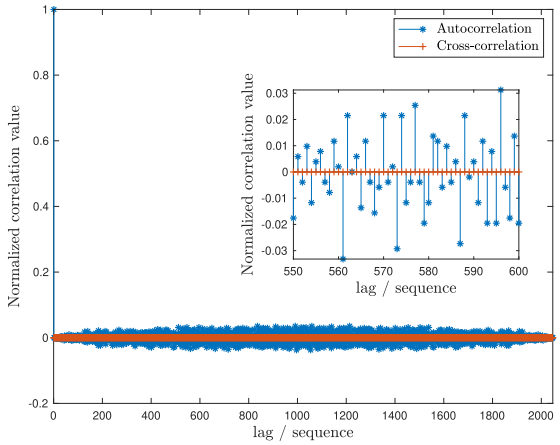

FIGURE 3. Autocorrelation and cross-correlation of the selected orthogonal m-sequence.

number of channel taps and sequence length only certain linear shifts yield a better result than the other. As the number of channel taps increases there is fewer sequence are suitable for the FDX operation.

The simulation is built in MATLAB using the system model as shown in Fig. 2. The channel coefficients are generated using improved Jake's model [36]. Due to a lack of actual model representing the self-interference available in the literature, we used the channel model used for the communication channel with different parameters. Both the channels introduce frequency selective fading. The average error of the estimators of both the channels is evaluated from 50 000 frames in the simulation over different noise levels in the communication link. The performance of the channel estimators was evaluated for different sequence lengths and different channel taps.

The channel estimation for the SI and communication channels are performed for different sequence length. Fig. 4 shows the mean square error (MSE) of the channel estimate with five channel taps each for different sequence length.

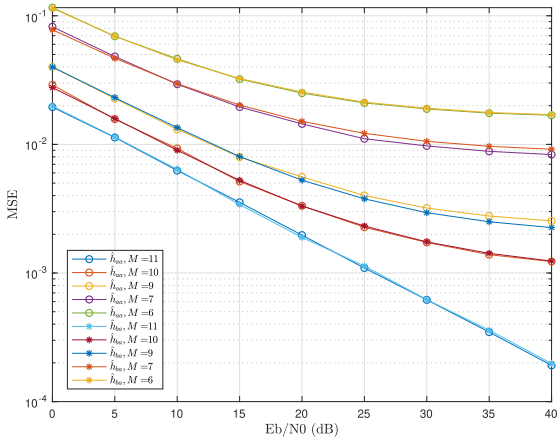

FIGURE 4. MSE of the channel estimates using different sequence length.

It can be observed the estimation error decreases with the increase in the sequence lengths since more information are available from usage of longer sequences. As the length of the pilot sequences increases, the performance of the estimation increases but saturates to the minimum error introduced by the sequence while performing the extraction and estimation.

The channel estimation for both SI and communication channels is performed for a different number of channel taps. Fig. 5 shows the MSE of the channel estimate for a different number of channel taps. Fig. 6 shows a close look on the MSE plots for different channel taps for a given noise level (15 dB). There is a noticeable increase in estimation error with the increase in channel taps resulting in more inter-symbol interference. The use of OFDM in the proposed method allowed mitigation of frequency selective fading to a set of parallel flat fading across the sub-carriers. This mitigation is limited to slow fading and the revision to handle fast fading is planned in the future works.

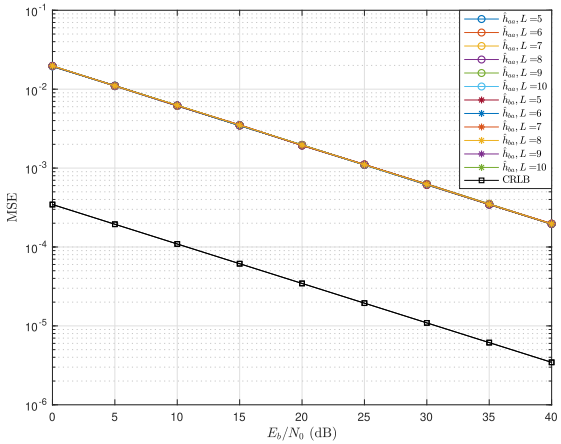

FIGURE 5. MSE of the channel estimation with CRLB for different channel taps and M = 11.

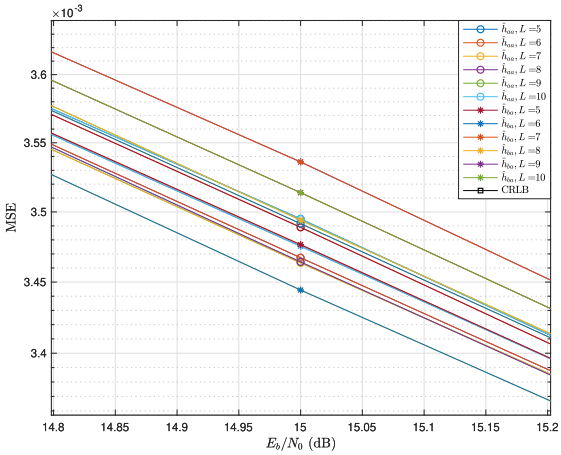

FIGURE 6. MSE of the channel estimation with CRLB for different channel taps and M = 11 (Zoomed).

In addition to the channel estimation error for different channel taps with sequence length is 2048 (M = 11),

the CRLB of the estimators is also plotted. The MSE of the estimate can get closer to the CRLB plot shown in Fig. 5, when the orthogonal sequence used can achieve the desired correlation property as discussed in Section III-C. The autocorrelation of the selected orthogonal m-sequence used is not zero for all its shifts. This deviation in the autocorrelation for certain shifts introduces error in addition to the noise which moves the MSE plots away from the CRLB. In addition, to both the channel estimator's CRLB being the same, it is also the CRLB for the channel estimator operated in half-duplex. Though both the FDX and HDX communication have the same bound and HDX achieving better performance, FDX excels in the bandwidth efficiency. The channel estimators of the HDX performs better than the FDX due to the absence of the SI but the bandwidth utilization of FDX is doubled compared to HDX.

The comparison of channel performance between HDX operation with FDX for different sequence alignments is shown in Fig.7. The pilot-based channel estimator was used in HDX same as that used in FDX operation. The FDX plots comprise of sequences with offsets reducing the cross-correlation between the pilot sequences. The offsets are introduced only to the far-end signal which is the signal of interest to be decoded. The plot comprises of three sets of channel estimation with no offset and two different offsets and compared with the HDX operation. The channel estimation performance of HDX and FDX with no offset aligns with each other since channels in FDX are orthogonal resulting HDX performance. In contrast, when the offsets get introduced the channel estimation of FDX degrades due to the loss of orthogonality and the performance saturates quickly with to the errors introduced. The estimation of SI channel suffers more due to error introduced by the poor cross-correlation with sequence from the far-end node. This implies the maximum channel estimation performance can be obtained only by maintaining the alignment of the sequence and preserving orthogonality.

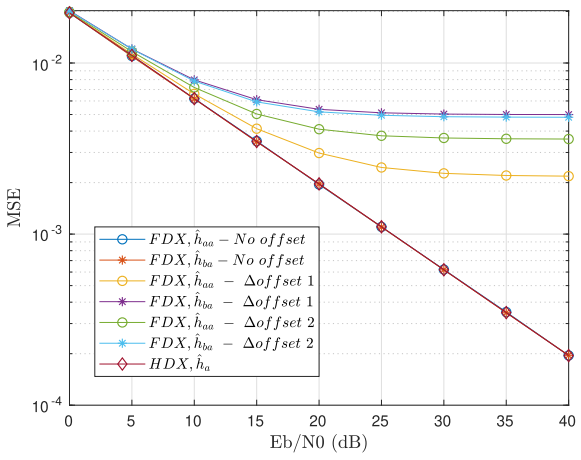

FIGURE 7. Comparison of channel estimation error between half-duplex and full-duplex with different sequence alignments.

VI. CONCLUSION

We demonstrated the separation and estimation of both self-interference and communication channels in full-duplex communication using the proposed method. The performance of the channel estimators depends on the correlation properties preserving the orthogonality and synchronization between the sequences. The deviation in cross-correlation affects performance of both the channel estimators. The effect on the performance depends on the which sequences not synchronized at the reception. The results of the theoretical limits of both the full-duplex estimators equal to half-duplex estimators shows the potential doubling of the spectral efficiency. Since the sequences are assigned to individual users, it can be reused in adjacent non-interfering cells. The proposed method can benefit the upcoming next-generation 5G and future generations of wireless communication where full-duplex operation considered to play a key role.

REFERENCES

[1] J. I. Choi, M. Jain, K. Srinivasan, P. Levis, P. Levis, S. Katti, "Achieving single channel, full duplex wireless communication details," in *Proc. 16th Annu. Int. Conf. Mobile Comput. Netw.*, 2010, pp. 1–12. [Online]. Available: https://sing.stanford.edu/site/publications/48

[2] W. Xiang, K. Zheng, and X. S. Shen, *5G Mobile Communications*. Springer, 2016.

[3] E. A. Makled, A. Yadav, O. A. Dobre, and R. D. Haynes, "Hierarchical full-duplex underwater acoustic network: A NOMA approach," in *Proc. OCEANS MTS/IEEE Charleston*, Oct. 2018, pp. 1–6.

[4] M. Mohammadi, X. Shi, B. K. Chalise, Z. Ding, H. A. Suraweera, C. Zhong, and J. S. Thompson, "Full-duplex non-orthogonal multiple access for next generation wireless systems," *IEEE Commun. Mag.*, vol. 57, no. 5, pp. 110–116, May 2019.

[5] T. M. C. Chu and H.-J. Zepernick, "Performance of a non-orthogonal multiple access system with full-duplex relaying," *IEEE Commun. Lett.*, vol. 22, no. 10, pp. 2084–2087, Oct. 2018.

[6] Z. Ding, P. Fan, and H. V. Poor, "On the coexistence between full-duplex and NOMA," *IEEE Wireless Commun. Lett.*, vol. 7, no. 5, pp. 692–695, Oct. 2018.

[7] B. Zheng, F. Chen, M. Wen, Q. Li, Y. Liu, and F. Ji, "Secure NOMA based cooperative networks with rate-splitting source and full-duplex relay," in *Proc. 15th Int. Symp. Wireless Commun. Syst. (ISWCS)*, Aug. 2018, pp. 1–5.

[8] I. A. Hemadeh, K. Satyanarayana, M. El-Hajjar, and L. Hanzo, "Millimeter-wave communications: Physical channel models, design considerations, antenna constructions, and link-budget," *IEEE Commun. Surveys Tuts.*, vol. 20, no. 2, pp. 870–913, 2nd Quart., 2018.

[9] L. Weizheng and T. Xiumei, "Throughput analysis of full-duplex network coding in two-way relay channel," in *Proc. IEEE 17th Int. Conf. Commun. Technol. (ICCT)*, Oct. 2017, pp. 85–90.

[10] H. Senol, X. Li, and C. Tepedelenlioglu, "Rapidly time-varying channel estimation for full-duplex Amplify-and-Forward one-way relay networks," *IEEE Trans. Signal Process.*, vol. 66, no. 11, pp. 3056–3069, Jun. 2018.

[11] D. Kim, H. Ju, S. Park, and D. Hong, "Effects of channel estimation error on full-duplex two-way networks," *IEEE Trans. Veh. Technol.*, vol. 62, no. 9, pp. 4666–4672, Nov. 2013.

[12] D. Korpi, L. Anttila, and M. Valkama, "Reference receiver based digital self-interference cancellation in MIMO full-duplex transceivers," in *Proc. IEEE Globecom Workshops (GC Wkshps)*, Dec. 2014, pp. 1001–1007.

[13] R. Keating, R. Ratasuk, and A. Ghosh, "Performance analysis of full duplex in cellular systems," in *Proc. IEEE 83rd Veh. Technol. Conf. (VTC Spring)*, May 2016, pp. 1–6.

[14] D. Lee and B.-W. Min, "2 × 2 MIMO in-band full-duplex radio front-end with 50 db self-interference cancellation in 90 mHz bandwidth," in *IEEE MTT-S Int. Microw. Symp. Dig.*, Jun. 2017, pp. 670–672.

[15] D. Liu, Y. Shen, S. Shao, Y. Tang, and Y. Gong, "On the analog self-interference cancellation for full-duplex communications with imperfect channel state information," *IEEE Access*, vol. 5, pp. 9277–9290, 2017.

[16] S. Khaledian, F. Farzami, B. Smida, and D. Erricolo, "Inherent self-interference cancellation at 900 MHz for in-band full-duplex applications," in *Proc. IEEE 19th Wireless Microw. Technol. Conf. (WAMICON)*, Apr. 2018, pp. 1–4.
[17] S.-I. C. Beamforming, M. B. Dastjerdi, N. Reiskarimian, T. Chen, G. Zussman, and H. Krishnaswamy, "Full duplex circulator-receiver phased array employing," in *Proc. IEEE Radio Freq. Integr. Circuits Symp. (RFIC)*, Jun. 2018, pp. 108–111.
[18] S. B. Venkatakrishnan, E. A. Alwan, and J. L. Volakis, "Wideband RF self-interference cancellation circuit for phased array simultaneous transmit and receive systems," *IEEE Access*, vol. 6, pp. 3425–3432, 2018.
[19] M. Duarte, C. Dick, and A. Sabharwal, "Experiment-driven characterization of full-duplex wireless systems," *IEEE Trans. Wireless Commun.*, vol. 11, no. 12, pp. 4296–4307, Dec. 2012.
[20] D. Bharadia, E. McMilin, and S. Katti, "Full duplex radios," *ACM SIGCOMM Comput. Commun. Rev.*, vol. 43, no. 4, pp. 375–386, Sep. 2013. [Online]. Available: http://dl.acm.org/citation.cfm?id=2534169.2486033
[21] Y. Li, L. Sun, C. Zhao, and L. Huang, "A digital self-interference cancellation algorithm based on spectral estimation in co-time co-frequency full duplex system," in *Proc. 10th Int. Conf. Comput. Sci. Edu. (ICCSE)*, Jul. 2015, pp. 412–415.
[22] A. M. M. Chandran and M. Zawodniok, "Transmitter leakage analysis when operating USRP (N210) in duplex mode," in *Proc. IEEE Int. Instrum. Meas. Technol. Conf. (IMTC)*, May 2015, pp. 340–345.
[23] L. Tian, S. Wang, Z. Cheng, and X. Bu, "All-digital self-interference cancellation in zero-if full-duplex transceivers," *China Commun.*, vol. 13, no. 11, pp. 27–34, Nov. 2016.
[24] Z. Luan, H. Qu, J. Zhao, and B. Chen, "Robust digital non-linear self-interference cancellation in full duplex radios with maximum correntropy criterion," *China Commun.*, vol. 13, no. 9, pp. 53–59, Sep. 2016.
[25] A. Masmoudi and T. Le-Ngoc, "A maximum-likelihood channel estimator for self-interference cancelation in full-duplex systems," *IEEE Trans. Veh. Technol.*, vol. 65, no. 7, pp. 5122–5132, Jul. 2016.
[26] J. Figwer, M. Michalczyk, and T. Glowka, "Accelerating the rate of convergence for LMS-like on-line identification and adaptation algorithms.—Part 1: Basic ideas," in *Proc. 22nd Int. Conf. Methods Models Autom. Robot. (MMAR)*, Aug. 2017, pp. 347–350.
[27] D. Korpi, M. AghababaeeTafreshi, M. Piilila, L. Anttila, and M. Valkama, "Advanced architectures for self-interference cancellation in full-duplex radios: Algorithms and measurements," in *Proc. 50th Asilomar Conf. Signals, Syst. Comput.*, Nov. 2016, pp. 1553–1557.
[28] M. Shammaa, H. Vogt, A. El-Mahdy, and A. Sezgin, "Adaptive self-interference cancellation for full duplex systems with auxiliary receiver," in *Proc. Int. Conf. Adv. Commun. Technol. Netw. (CommNet)*, Apr. 2019, pp. 1–8.
[29] Y. K. Hua and W. Chang, "Time shifted pilots scheme for full-duplex massive MIMO systems," *IEEE Trans. Veh. Technol.*, vol. 68, no. 3, pp. 3022–3026, Mar. 2019.
[30] H. Xing, D. Wei, and F. Yin, "Channel estimation using orthogonal superimposed pilot for MIMO systems," in *Proc. 2nd Int. Conf. Signal Process. Syst.*, Jul. 2010, pp. 625–628.
[31] H. Wang, Y. Huang, S. Jin, Y. Du, and L. Yang, "Pilot contamination reduction in multi-cell TDD systems with very large MIMO arrays," *Wireless Pers. Commun.*, vol. 96, no. 4, pp. 5785–5808, Oct. 2017.
[32] Y. Wu, T. Liu, M. Cao, L. Li, and W. Xu, "Pilot contamination reduction in massive MIMO systems based on pilot scheduling," *EURASIP J. Wireless Commun. Netw.*, vol. 2018, no. 1, p. 21, Jan. 2018.
[33] X. Hou, C. Gao, Y. Zhu, and S. Yang, "Detection of active attacks based on random orthogonal pilots," in *Proc. 8th Int. Conf. Wireless Commun. Signal Process. (WCSP)*, Oct. 2016, pp. 1–4.
[34] G. T. Bura as and G. M. Boynton, "Efficient design of event-related fMRI experiments using M-sequences," *NeuroImage*, vol. 16, no. 3, pp. 801–813, Jul. 2002.
[35] S. M. Kay, "Fundamentals of statistical signal processing," in *Prentice-Hall Signal Processing Series*. 1993.
[36] C. Xiao, Y. Zheng, and N. Beaulieu, "Novel sum-of-sinusoids simulation models for Rayleigh and rician fading channels," *IEEE Trans. Wireless Commun.*, vol. 5, no. 12, pp. 3667–3679, Dec. 2006.

ARUL MATHI MARAN CHANDRAN (Graduate Student Member, IEEE) received the B.Tech. degree in electronics and communication engineering from Pondicherry University, India, in 2008, and the M.S. degree in electrical engineering from the Missouri University of Science and Technology, Rolla, MO, USA, in 2015, where he is currently pursuing the Ph.D. degree in electrical engineering.

In 2008, he joined MBIT Wireless Pvt., Ltd., Chennai, India, where he worked on ASIC front-end development for WiMAX and LTE. In 2013, he joined Qualcomm, Chennai, where he worked on verification efforts for USB3 development. His current research interests include communication systems, wireless networks, software-defined radios, and embedded systems.

Mr. Chandran is a member of the Tau Beta Pi and the Eta Kappa Nu honor societies.

LEI WANG (Member, IEEE) received the M.S. degree from the Beijing University of Chemical Technology, China, in 2005, and the Ph.D. degree in computer engineering from the Missouri University of Science and Technology, in 2017.

After graduating with the M.S. degree, he was an Embedded Software Engineer with the Beijing Office, SYS TEC electronic GmbH. Upon graduation with the Ph.D. degree, he was a Visiting Assistant Professor with the Union College. He is currently an Assistant Professor with the Computer Science Department, University of Wisconsin–La Crosse. His research interests include localization, sensor fusion, machine learning, wireless communications, and wireless sensor/ad hoc networks.

MACIEJ ZAWODNIOK (Senior Member, IEEE) received the M.Sc. degree in computer science from the Silesian University of Technology, Gliwice, Poland, in 1999, and the Ph.D. degree in computer engineering from the Missouri University of Science and Technology, Rolla, MO, USA, in 2006.

He has been with the Missouri University of Science and Technology, since 2008, where he is currently an Assistant Professor of computer engineering and an Assistant Director of the NSF I/UCRC on intelligent maintenance systems. He has coauthored over 20 peer-reviewed journal articles and book chapters and over 40 refereed IEEE conference papers. His current research interests include adaptive and energy-efficient protocols for wireless networks, network-centric systems, network security, and cyber-physical and embedded systems with applications to manufacturing and maintenance.

Dr. Zawodniok was a recipient of the prestigious NSF CAREER Award on wireless networking using passive communication systems, in 2010.